



CANADA

01-7991622

THE CALCULATION OF THE PORE
SIZE DISTRIBUTION FROM THE
NITROGEN DESORPTION ISOTHERM

DEPARTMENT OF MINES AND
TECHNICAL SURVEYS, OTTAWA

MINES BRANCH
TECHNICAL BULLETIN

TB 26

Price 25 cents.

W. D. MACHIN, B. I. PARSONS
& D. S. MONTGOMERY

FUELS AND MINING PRACTICE DIVISION

DECEMBER 1961

Mines Branch Technical Bulletin TB 26

THE CALCULATION OF THE PORE SIZE DISTRIBUTION
FROM THE NITROGEN DESORPTION ISOTHERM

by

W. D. Machin*, B. I. Parsons**

and

D. S. Montgomery***

- - - -

SYNOPSIS

An apparatus is described for the determination of the adsorption-desorption isotherms of nitrogen on pellets of catalyst. Three methods of calculating the pore size distribution from the desorption isotherms are compared on three samples. The results of the investigation indicate that the best method of determining the pore size distribution is by a numerical integration of the desorption data. The other methods, although faster and easier, can result in a misleading distribution.

*Technical Officer, **Senior Scientific Officer and ***Senior Scientist, Fuels and Mining Practice Division, Mines Branch, Department of Mines and Technical Surveys, Ottawa, Canada.

Bulletin technique de la Direction des Mines TB 26

CALCUL DE LA DISTRIBUTION DIMENSIONNELLE
DES PORES D'APRÈS L'ISOTHERME DE DÉSORPTION D'AZOTE

par

W.D. Machin*, B.I. Parsons**

et

D.S. Montgomery***

RÉSUMÉ

Ce bulletin décrit un appareil pour déterminer les isothermes d'adsorption-désorption d'azote par des boulettes de catalyseurs. Trois échantillons servent à comparer trois méthodes de calcul de la distribution dimensionnelle des pores d'après les isothermes de désorption. Il ressort des résultats de cette étude que la meilleure méthode de calcul de la distribution dimensionnelle des pores consiste à intégrer numériquement les résultats de désorption. Quoique plus rapides et faciles, les autres méthodes peuvent donner une distribution trompeuse.

*Agent technique, **Chargé de recherche principal et ***Scientiste principal, Division des combustibles et des techniques de l'exploitation minière, Direction des mines, ministère des Mines et des Relevés techniques, Ottawa, Canada.

CONTENTS

	<u>Page</u>
Synopsis	i
Résumé	ii
Introduction	1
Historical Background	2
Apparatus and Experimental Procedure	9
Experimental Results	13
The Calculation of the Pore Size Distribution	16
1. Method of Oulton	16
2. Method of Wheeler and Shull	17
3. Method of Barrett, Joyner and Halenda.....	23
Results of the Calculations, and Discussion.....	28
References.....	35

FIGURES

<u>No.</u>		<u>Page</u>
1.	Typical adsorption and desorption isotherms	4
2.	The principal radii of curvature of the meniscus in filled and unfilled capillary pores	6
3.	The Brunauer, Emmett and Teller nitrogen adsorption apparatus	10
4.	Nitrogen adsorption-desorption isotherms for the Union Oil catalyst	14
5.	Nitrogen adsorption-desorption isotherms for the Nalcat and K-536 catalysts	15
6.	Standard inverted isotherms for a Maxwellian distribution of pore sizes	20
7.	Standard inverted isotherms for a Gaussian distribution ($B = 2$) of pore sizes	21
8.	Standard inverted isotherms for a Gaussian distribution ($B = 5$) of pore sizes	22
9.	Plot of the corrected Kelvin radius versus the relative pressure	26
10.	Graphs of n and R for the numerical integration ...	27
11.	The pore volume distribution in the Union Oil catalyst as manufactured	29
12.	The pore volume distribution in the reactivated Union Oil catalyst	30
13.	The pore volume distribution in the K-536 catalyst	31
14.	The pore volume distribution in the Nalcat catalyst	32
15.	The surface area distribution	33

INTRODUCTION

Many modern refining techniques, which involve chemical transformations, depend upon porous catalysts or catalytic substances supported on porous media. The vaporized petroleum is usually passed through a bed of solid pellets in a flow system. To attain rates of conversion that are economically acceptable with low catalyst losses, great care must be taken in the selection and preparation of the support as well as in the choice of the active catalytic substance. The surface area and the pore size distribution--which are the characteristics of the catalyst most influenced by the manner of preparation--can affect both the activity of the ingredients and the accessibility of the surface to the reaction mixture. One method of measuring the surface area which has gained wide acceptance is that of Brunauer, Emmett and Teller (BET)(1)*. This technique has become generally recognized as a highly reproducible method of measuring the surface area of a wide variety of porous substances. Several attempts have also been made to extend these measurements to give an estimate of the most probable pore size distribution.

The purpose of the present bulletin is two-fold: First, to describe briefly an apparatus for the measurement of the nitrogen

*References are listed at the end of the bulletin, in the order in which they are numbered.

adsorption and desorption isotherms by the BET method; and, second, to compare the various methods of calculating the pore size distribution from these isotherms. This report was originally designed for the instruction of summer students and others assisting in the catalytic research of this Division. The porous materials selected for the investigation were three catalysts currently in use in the Division for the hydrodesulphurization of a coker distillate derived from Alberta bitumen: (a) the Union Oil Company of California type N-H 760 cobalt molybdate catalyst, (b) a similar cobalt molybdate catalyst manufactured by the National Aluminate Company of Chicago, Illinois, and (c) a clay-supported catalyst made in Germany during World War II for the hydrogenation of heavy oils.

HISTORICAL BACKGROUND

The nitrogen adsorption method of determining surface areas was proposed in its most practical form by Brunauer, Emmett and Teller in 1938 (1). The first step in the BET procedure is to heat a sample of the solid under vacuum until all the adsorbed gases are removed. After the de-gassing process, the sample vessel is cooled to approximately -196°C in a Dewar flask containing boiling nitrogen at atmospheric pressure. The amount of nitrogen adsorbed by the sample material at this temperature is then measured at various pressures up to the saturation pressure. Under the conditions of the experiment the saturation pressure of nitrogen is usually very close

to atmospheric pressure. Slight deviations from atmospheric pressure are caused by the presence of impurities, principally dissolved oxygen, in the liquid nitrogen surrounding the sample vessel. The presence of impurities raises the boiling temperature of this liquid nitrogen.

The most convenient means of recording the experimental data is as an isotherm, in which the volume adsorbed is plotted as a function of the ratio of the applied pressure to the saturation pressure. Typical adsorption and desorption isotherms are shown in Figure 1. The lower curves in Figure 1 are the adsorption isotherms measured by progressively increasing the pressure of nitrogen from zero to the saturation pressure. The upper curves are desorption isotherms, determined by first saturating the sample with nitrogen and then systematically lowering the pressure and measuring the nitrogen evolved.

The calculation of the surface area is based upon the adsorptive branch of the isotherm as applied to the Brunauer, Emmett and Teller equation for multilayer adsorption:

$$\frac{P}{V(P_0 - P)} = \frac{1}{V_m C} + \frac{C-1}{V_m C} P/P_0$$

where P and P_0 are the equilibrium pressure and the saturation pressure, respectively, of nitrogen at the temperature of boiling liquid nitrogen at one atmosphere,

V is the volume adsorbed at the pressure P
(ml STP per gram of solid adsorbent),

V_m is the volume of nitrogen corresponding to one complete monolayer of adsorbed gas
(ml STP per gram of solid adsorbent), and

C is a constant.

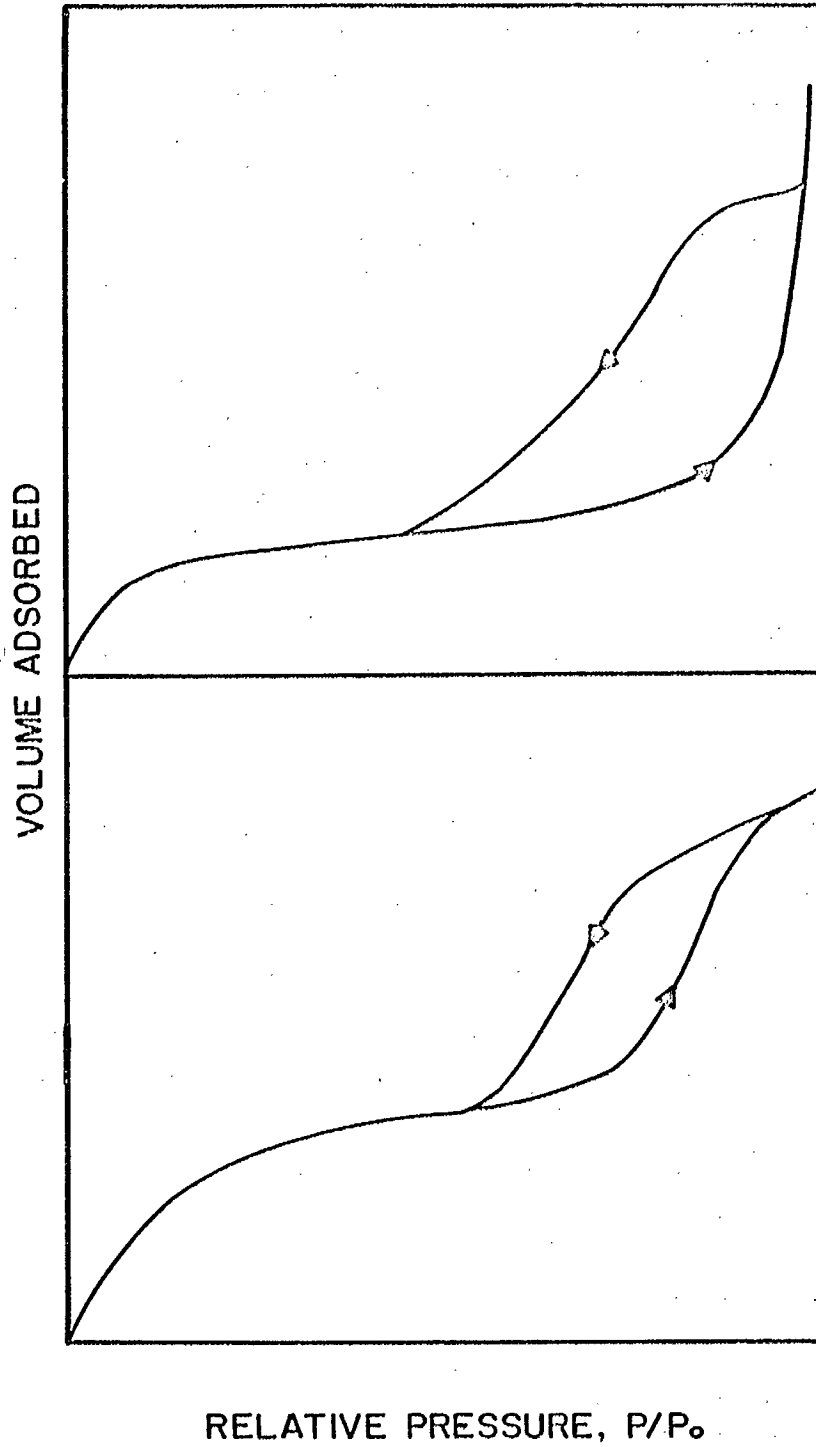


Figure 1. Typical adsorption and desorption isotherms.

For most substances, the BET equation applies reasonably well in the relative pressure range 0.05 to 0.35. In this range a plot of

$$\frac{P}{V(P_0 - P)} \quad \text{vs} \quad P/P_0$$

is very nearly a straight line. The value of V_m , the monolayer volume, can be calculated from the intercept and slope of this line. The surface area of the sample is calculated from V_m , assuming the area of the nitrogen molecule is $16.2 (\text{\AA})^2$.

The calculation of the pore size distribution is based upon the measurements made at high relative pressures in the region of the hysteresis loop. The theory of the hysteresis loop is fundamentally an extension of Lord Kelvin's theory (3) of the relation between droplet size, surface tension and vapour pressure. Kelvin originally proposed his theory to explain the experimental observation that the vapour pressure of a liquid is greater when in the form of small drops than when it has a plane surface. In the case of condensation within a pore, the curved surfaces responsible for the elevation of the vapour pressure are associated with liquid surfaces within the pore. The radii of curvature of these surfaces depend on the quantity of liquid in the pore, as may be seen in Figure 2. In an unfilled, cylindrical pore the more material that condenses in the capillary, the smaller the radius of curvature becomes. Also, in the case of an unfilled cylindrical pore, only one radius of curvature is involved--that of

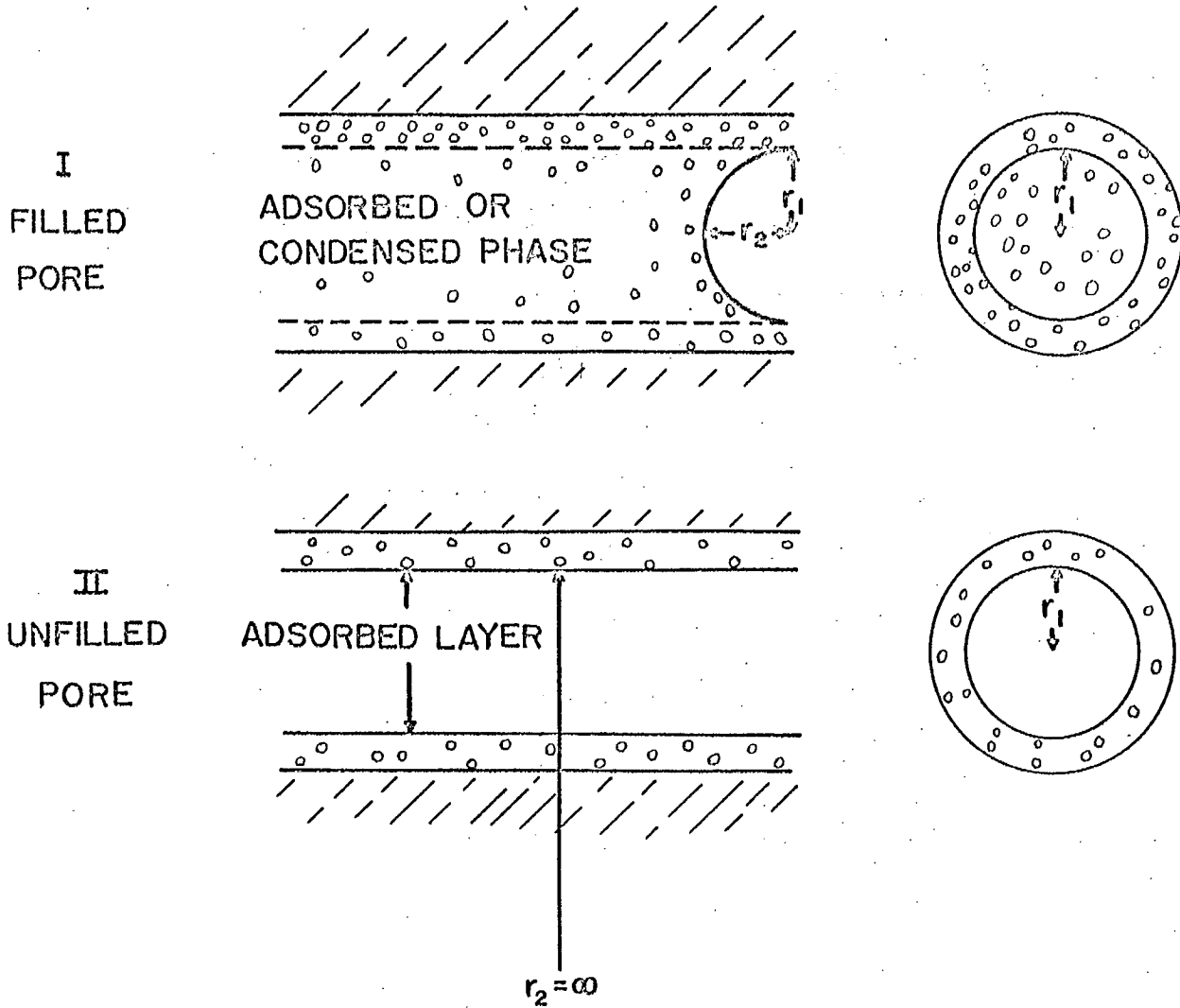


Figure 2. The principal radii of curvature of the meniscus in filled and unfilled capillary pores.

the circular wall of the "pipe" formed as gas condenses. In a filled pore, on the other hand, the meniscus is hemispherical, involving two radii of curvature. Using these concepts, Carman (4) has extended the Kelvin theory and has derived the following equation:

$$RT \ln P/P_0 = -S_t V_M \left[\frac{1}{r_1} + \frac{1}{r_2} \right] \cos a$$

where S_t is the surface tension of the adsorbate,

V_M is the molar volume of the condensed gas,

a is the angle of contact of the condensate with the pore wall*, and

r_1 and r_2 are the principal radii of curvature of the meniscus in the capillary shown in Figure 2.

The Carman equation is similar to the Kelvin equation for spherical droplets except that the effect of the surface tension and curvature upon the vapour pressure is to decrease it relative to a plane surface of the same liquid. This is indicated by the negative sign in the Carman equation. The reason for the elevation of the equilibrium partial pressure for droplets and the decrease in the equilibrium partial pressure for adsorbed liquid layers in pores is as follows: In a spherical droplet the curvature of the surface is toward the centre of the liquid drop, and the surface tension acts to compress the liquid phase. This compression elevates the equilibrium partial pressure of the liquid in the gas phase above that which would be in equilibrium with a plane surface of the same liquid. On the other hand, when the liquid is distributed over the interior of a

*Since multilayer adsorption usually precedes condensation, $\cos a$ is generally assumed to be unity.

cylindrical pore the curvature of the liquid surface is toward a centre located in the gas phase. The surface tension forces now tend to decrease the pressure on the liquid phase and to reduce the equilibrium partial pressure of the liquid in the gas phase as compared with that in equilibrium with a plane surface of the same liquid.

In a porous solid the vapour pressure over the adsorbed or condensed phase in an unfilled pore decreases as the pore narrows, until eventually the pore fills. When the pore is completely filled, the only liquid surface open to the system is the hemispherical meniscus at the end of the pore. Then, during the desorption cycle, to empty the pore the pressure must be lowered to a value less than that required to completely fill it. For the filled pore $r_1 = r_2$ and the Kelvin-Carman equation becomes:

$$RT \ln P/P_0 = \frac{-2 S_t V_M}{r}$$

The most important point to understand is that, during the desorption cycle, when the vapour pressure for the meniscus at the pore mouth is reached the pore empties itself of condensed gas. Once the meniscus is broken, the condensed phase on the cylindrical pore walls can exist only at a higher pressure, and the condensate evaporates to the concentration corresponding to multilayer adsorption at that specific pressure. The gas evolved between two selected pressures is, therefore, a measure (subject to correction for adsorption) of the pore volume within the corresponding limits of pore radius.

APPARATUS AND EXPERIMENTAL PROCEDURE

The apparatus used is shown schematically in Figure 3. This is a standard BET nitrogen adsorption apparatus, and has been fully described by others, e. g. Joyner (5) and Bugge and Kerloguc (6).

The principal parts of the apparatus were:

- (1) a gas burette to measure the volume of gas adsorbed,
- (2) an oxygen vapour pressure thermometer,
- (3) a manometer to measure adsorption pressure,
- (4) a sample bulb, and
- (5) traps for purifying the gases used.

A weighed sample of the material to be investigated was sealed into the apparatus and baked out overnight, under vacuum, at 200°C to remove the physically adsorbed gases and vapours.* When the baking operation was completed, the sample vessel and the thermometer bulb were cooled in liquid nitrogen. For the adsorption branch of the isotherm, measured quantities of nitrogen were added to the gas burette, and the volume of nitrogen adsorbed was noted periodically up to the saturation pressure. At the saturation pressure, the order of the measurements was reversed for the desorption isotherm. The pressure over the sample was reduced by lowering the level of the mercury in the burette, and the volume of gas desorbed was measured at selected intervals of pressure. Desorption was continued until the pressure of nitrogen over the sample was negligible.

*Small amounts of some chemisorbed materials may still be left on the surface.

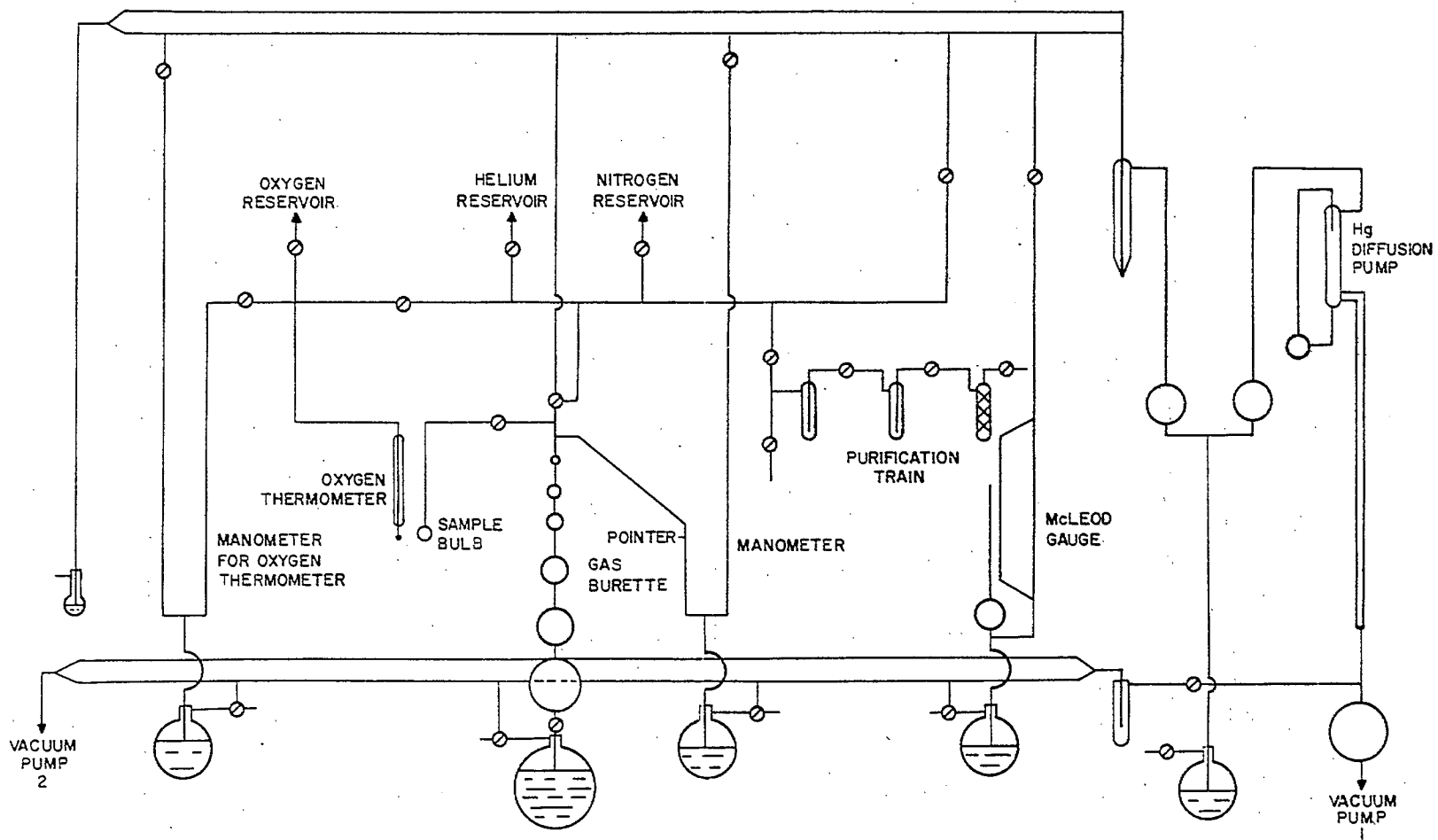


Figure 3. The Brunauer, Emmett and Teller nitrogen adsorption apparatus.

The temperature of the sample was measured as a function of the vapour pressure of the liquid oxygen in the adjacent bulb. The overall temperature varied slightly from experiment to experiment, due to variations in the atmospheric pressure and to condensation of oxygen from the atmosphere into the Dewar flask surrounding the sample. Very little could be done to compensate for fluctuations in the atmospheric pressure except to measure the changes and to allow for them. Variations due to the condensation of oxygen, however, could be reduced considerably by closing the neck of the Dewar flask with a loose wad of glass wool. The evaporating nitrogen sweeping through the passages in the glass wool prevented the diffusion of air back down into the flask.

The deadspace of the sample vessel--that is, the volume of the bulb not occupied by the solid material--was determined with helium at the temperature of liquid nitrogen.

Three catalysts were selected for study. The first was a cobalt molybdate catalyst, on an alumina-silica support, manufactured by the Union Oil Company of California. Two experiments were made with this particular catalyst: (a) with the material as supplied by the company, and (b) with a batch that had been used and regenerated several times in the Mines Branch hydrogenation pilot plant.

The second catalyst investigated was a cobalt molybdate catalyst, on a pure alumina support, manufactured by the National Aluminate Corporation, of Chicago. The third material was a clay-

base catalyst prepared in Germany during World War II for the vapour-phase hydrogenation of heavy hydrocarbon fractions derived from coal. The experiments with both of these were made using the materials as received from the manufacturer. The German catalyst was considered by the Allied investigating teams to be the most satisfactory single catalyst for the production of synthetic liquid fuel in the vapour-phase step of coal hydrogenation. It was developed by the Botrop Wellheim plant of I.G. Farbenindustrie, and its code number was K-536.

EXPERIMENTAL RESULTS

Two experiments were made with two separate portions of Union Oil catalyst. The first experiment was made with the cobalt molybdate catalyst as supplied by the Union Oil Co. The second experiment was made with a batch of the catalyst used and regenerated several times in the Mines Branch pilot plant. The results of the adsorption and desorption measurements made on the two samples of the Union Oil Company cobalt molybdate catalyst are shown in Figure 4. The two isotherms are very nearly identical. The hysteresis loops begin and close at almost the same relative pressures, indicating little change in the structure of the catalyst with activation or regeneration.

The isotherms for the National Aluminate catalyst (trade name "Nalcat") and for the German K-536 catalyst are shown in Figure 5. The shape of the curves obtained with the German material differed considerably from the type of result obtained with the other catalysts. In the case of the alumina-based or alumina-silica-based catalysts, it was possible to approach the pressures at which the hysteresis loop closed, with reasonable accuracy. With the clay catalyst, however, the saturation pressure could only be approached asymptotically, and it was not possible to obtain a clearly defined pressure at which the desorption isotherm began to differ from the adsorptive branch.

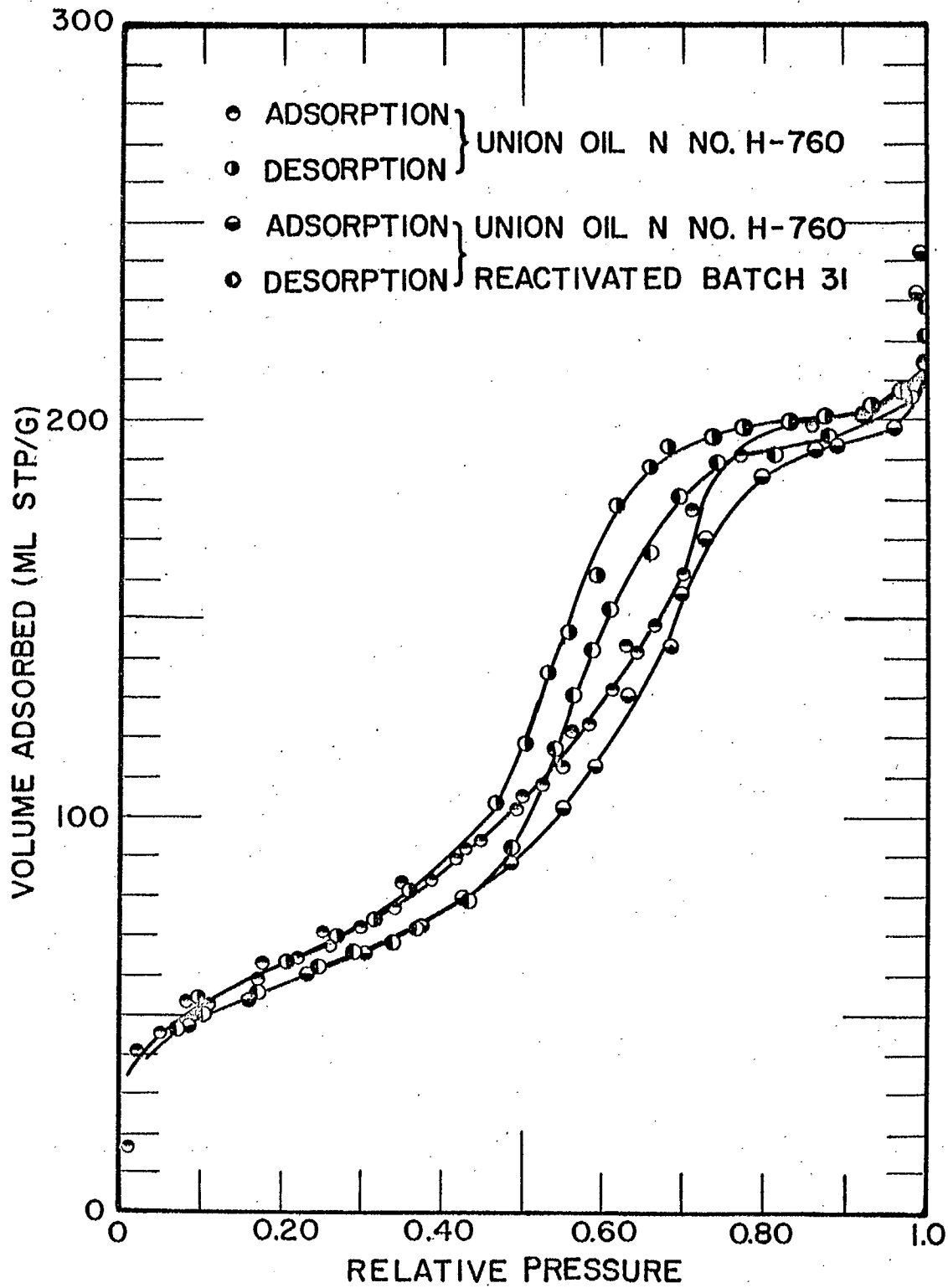


Figure 4. Nitrogen adsorption-desorption isotherms for the Union Oil catalyst.

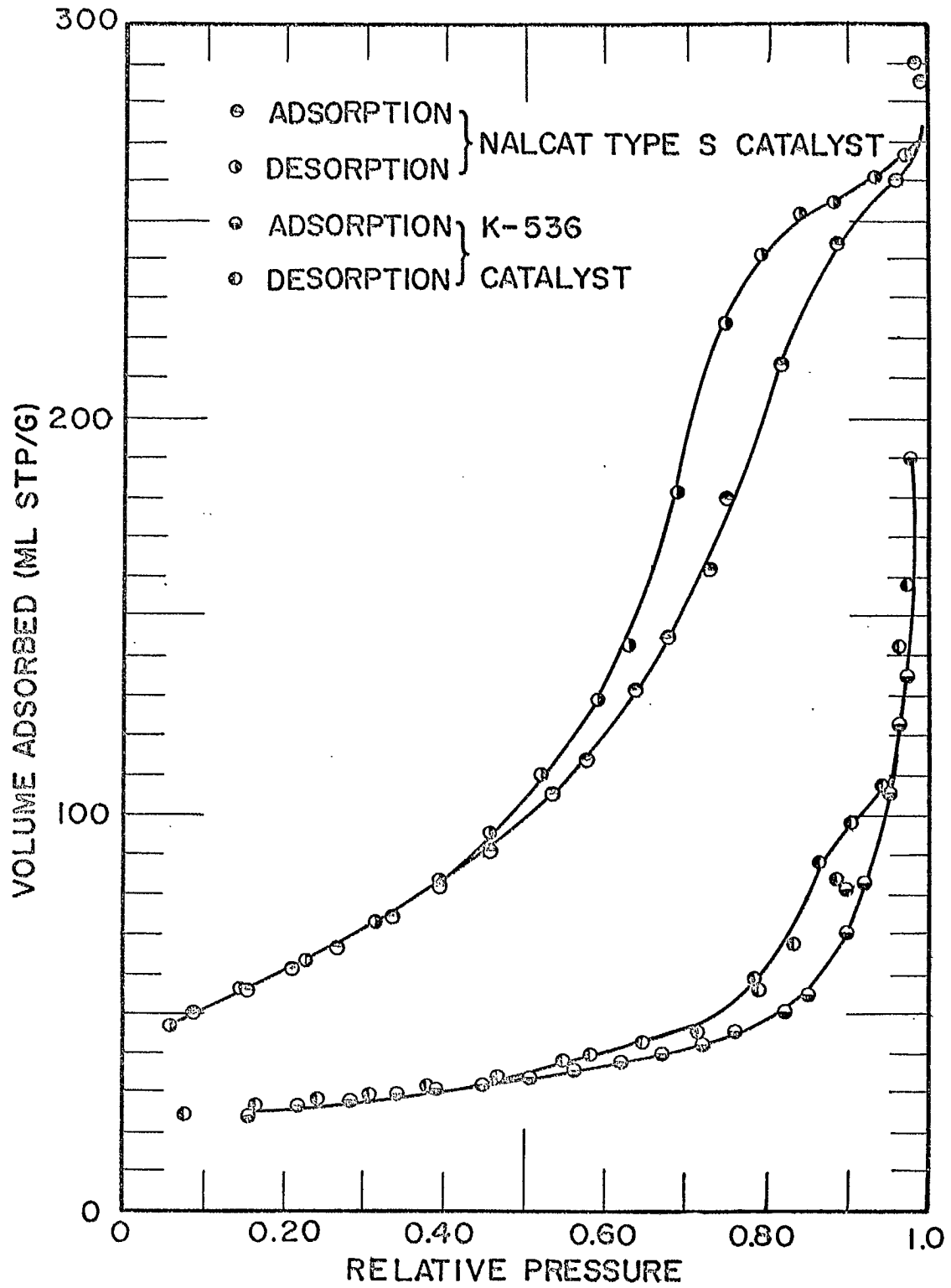


Figure 5. Nitrogen adsorption-desorption isotherms for the Nalcat and K-536 catalysts.

THE CALCULATION OF THE PORE SIZE DISTRIBUTION

1. Method of Oulton

The earliest attempt to derive a pore size distribution from the desorption isotherm was made by Anderson (7). He suggested that all adsorption was due to capillary condensation, and calculated the pore size distribution directly from the Kelvin-Carman equation.

Oulton (8) improved the accuracy of this type of calculation by adding a correction to the radius figures to allow for multilayer adsorption. Oulton considered all adsorption to be physical adsorption on the walls up to the inception of the hysteresis loop. Beyond the inception of the loop, all adsorption was supposed to be due to capillary condensation. The radius of the bare-walled pore, r_c , then becomes:

$$r_c = r_k + t$$

where r_k is the Kelvin radius, and t is the thickness of a monolayer.

The thickness of the adsorbed film, t , is determined from the relation:

$$4.2 \frac{V_H}{V_m} = t$$

where V_H is the volume of gas adsorbed per gram of substrate up to the beginning of the hysteresis loop, and V_m is the monolayer volume of gas as calculated from the BET equation. The quantity 4.2 is the thickness, in Ångström units, of one physically adsorbed layer of nitrogen. The procedure for the calculation was as follows:

- (a) The desorptive branch of the isotherm was plotted as the volume adsorbed versus r_c , the corrected radius.
- (b) Tangents were drawn at regular intervals of radius on the above curve. The graph of the value of these tangents, dV/dr_c , versus r_c gives the pore volume distribution for the solid as a function of the pore radius.

2. Method of Wheeler and Shull

Quite a different approach to the calculation of the pore size distribution has been proposed by Wheeler (9). Essentially, his method consisted of the comparison of theoretical and experimental isotherms.

From first principles, Wheeler calculated the theoretical shape of the adsorption-desorption isotherm for specific types of pore size distributions. For each type, the parameters in the calculated distribution can be altered in a stepwise manner until the theoretical isotherm agrees reasonably well with the experimental curve. The type of distribution is decided by the general shape of the experimental isotherm, and the parameters are established by the numerical data.

The Wheeler theory is summarized in the equation:

$$V_g - V_a = \pi \int_{R_p}^{\infty} (r-t)^2 L(r) dr$$

where V_g is the total pore volume in ml STP/g,

V_a is the volume of the adsorbed phase present in the sample at any relative pressure,

R_p is the radius of the largest filled pore at that relative pressure,

t is the multilayer thickness adsorbed at the relative pressure,

$L(r) dr$ is the total length of pores whose radii fall between r and $r + dr$, and

$V_g - V_a$, at a pressure P , is equal to the total volume of the pores that have not been filled.

Wheeler corrected his radius figures to allow for the thickness of the adsorbed gases in the pores that were free of condensation:

$$R_p = t - \frac{2 S_t V_M}{RT \ln P/P_0}$$

The values for t in the calculation of the corrected radius were taken from the BET theory for multilayer adsorption. Wheeler's correction to the Kelvin radius differs from that proposed by Oulton, in that t is dependent on the relative pressure. In the Oulton type of calculation, t is a fixed quantity dependent only on the inception of the hysteresis loop.

The general method of comparing theoretical with experimental curves was put into a more convenient form by Shull in 1948 (10). He represented the pore size distribution by a series of purely mathematical equations of the Maxwellian or Gaussian type and published a set of graphs of the effect of small changes in the parameters. He assumed the Maxwellian type of distributions to be of the form:

$$L(r) = A r e^{-r/r_0}$$

where A and r_0 are constants.

Shull substituted this expression for $L(r)$ into the Wheeler equation and, after considerable re-arrangement and simplification, derived the equation:

$$V_g - V_a = Ar_o^4 M(R, r_o)$$

He then calculated the value of the function represented by $M(R, r_o)$ for separate values of R and r_o and published the results as "standard" isotherms, shown in Figure 6.

Similarly, the Gaussian distribution of pore length was assumed to be of the form:

$$L(r) = Ae^{-\left[B/r_o(r - r_o)\right]^2},$$

which upon substitution into the Wheeler equation becomes:

$$V_g - V_a = 2A (r_o^3/B)G_B(R, r_o)$$

Shull determined $G_B(R, r_o)$ for $B = 2$ and $B = 5$ and various values of R and r_o . These "standard" isotherms are shown in Figures 7 and 8. The parameter B controls the width of the distribution. For $B = 2$ the distribution is very sharp, and for $B = 5$ the distribution is relatively broad.

Shull also improved upon Wheeler's correction for the radius of the pore by experimentally determining the relation between t and P/P_o . His experiments showed that Wheeler's correction figures, calculated from BET theory, were too large at high relative pressures.

The procedure used at the Mines Branch for the "Shull" distribution calculations was as follows: The desorption data were plotted as $V_g - V_a$ (log scale) versus r_c , the corrected Kelvin radius. This curve was then compared with the standard isotherms shown in Figures 6, 7 and 8. The pore size distribution was known immediately from the parameters of the standard isotherm. As many

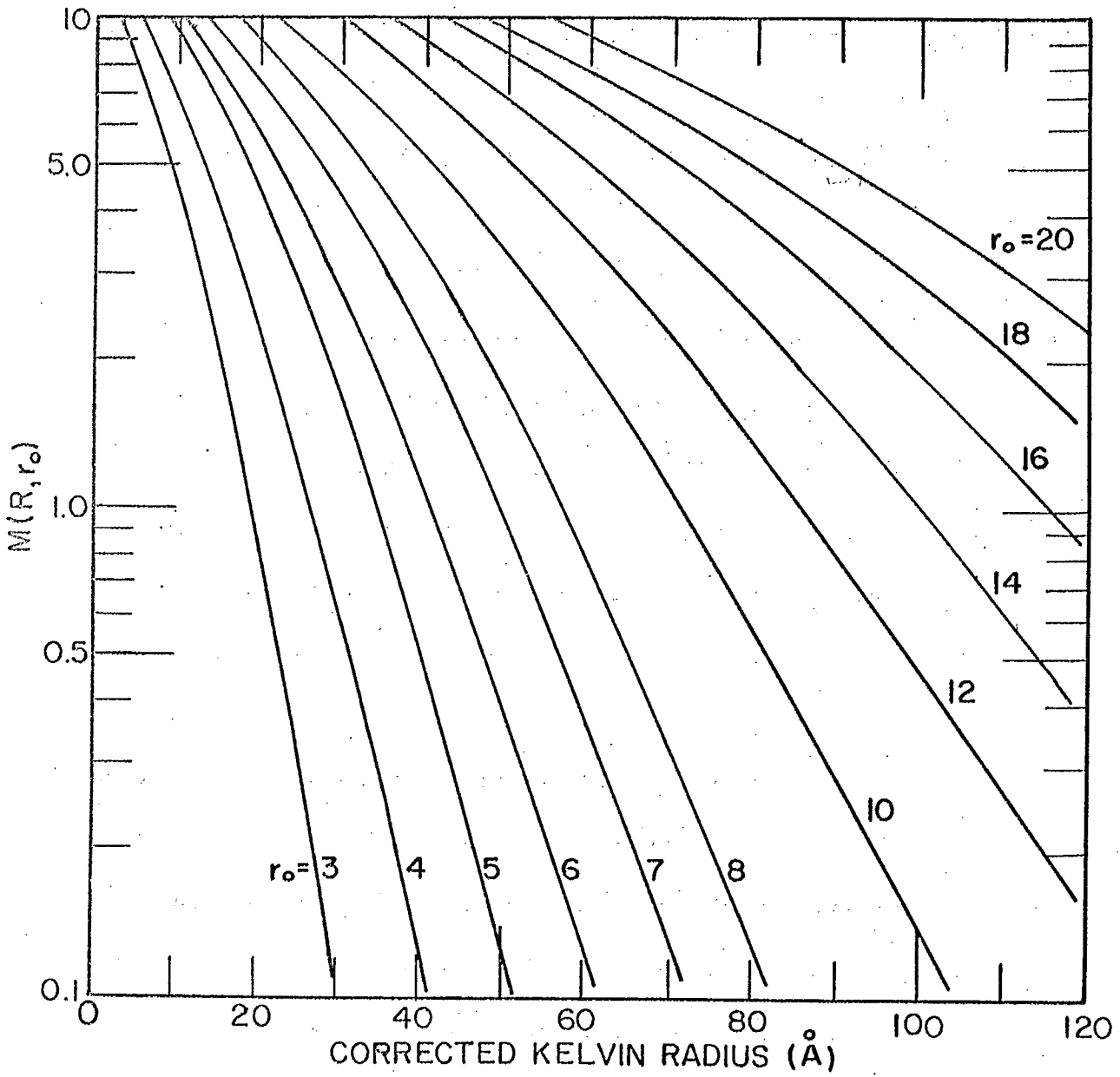


Figure 6. Standard inverted isotherms for a Maxwellian distribution of pore sizes.

(From Shull (10))

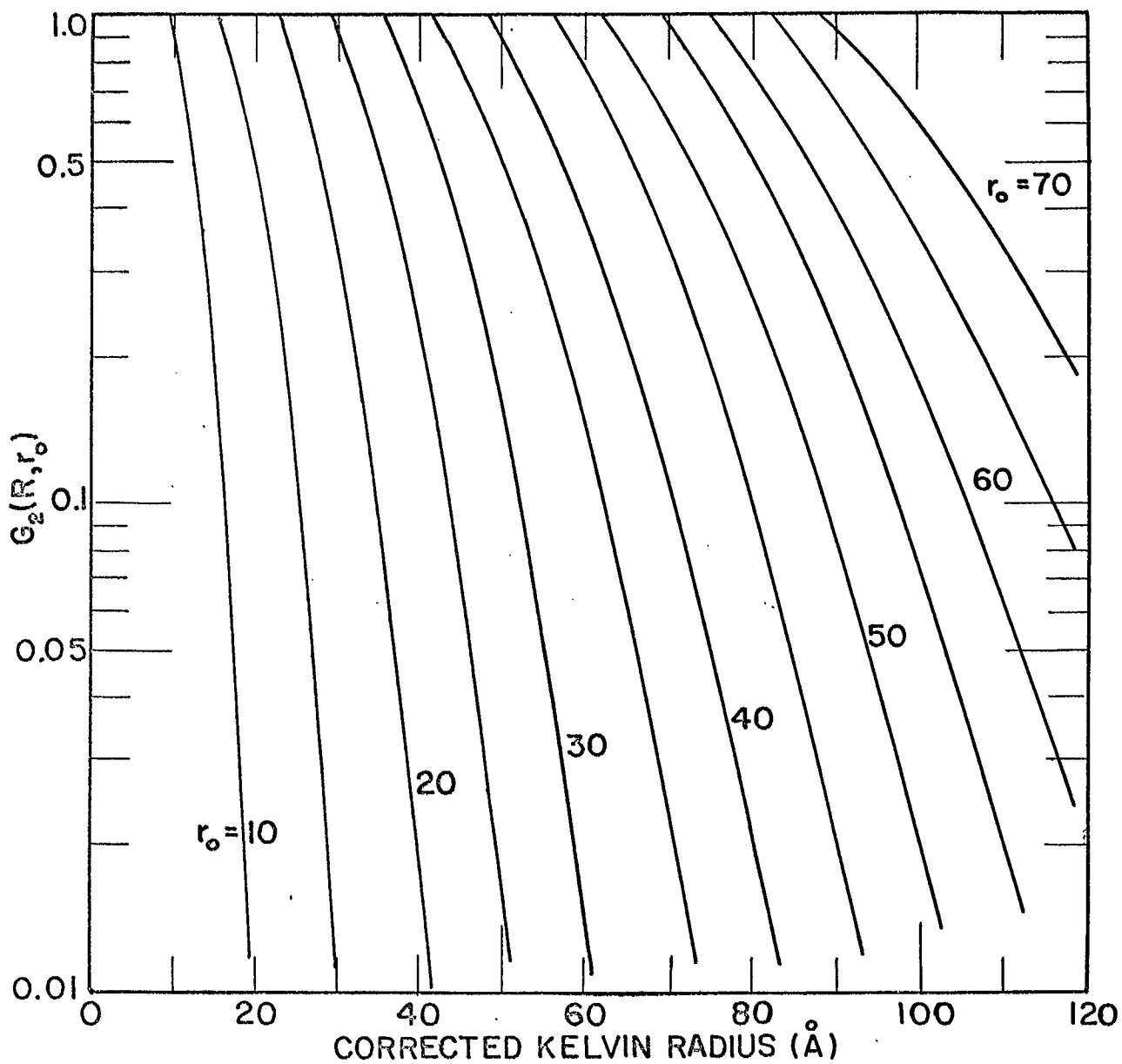


Figure 7. Standard inverted isotherms for a Gaussian distribution ($B = 2$) of pore sizes.

(From Shull (10)).

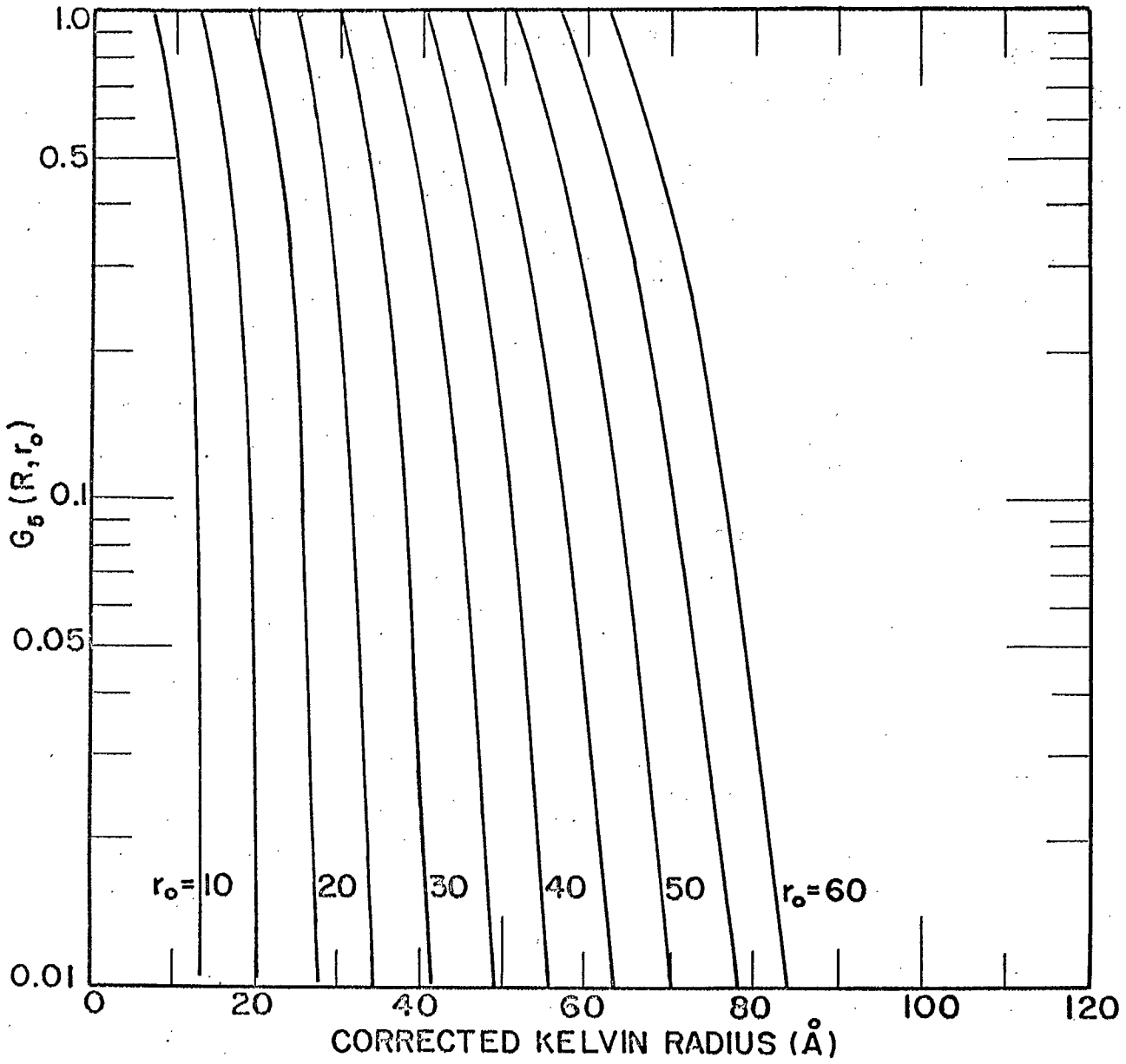


Figure 8. Standard inverted isotherms for a Gaussian distribution ($B = 5$) of pore sizes.

(From Shull (10))

component isotherms were used as were necessary to bring about the the desired accuracy.

3. Method of Barrett, Joyner and Halenda

Barrett, Joyner and Halenda (BJH) (11) have proposed a numerical integration of Wheeler's equation as a means of determining the pore size distribution. This technique has the advantage that it is dependent only on the experimental data. The original method proposed for the integration involved the selection of a somewhat arbitrary constant. Pierce later improved and simplified the procedure in a paper published in 1953(12). The procedure described below is essentially that proposed by Pierce.

The calculations were begun by replotting the isotherm as the volume desorbed against the corrected Kelvin radius, r_c , where, as before:

$$r_c = r_k + 4.2 n$$
$$r_k = \frac{-4.14}{\log P/P_0} \quad \text{and} \quad n = \frac{V_H}{V_m}$$

The curve was then divided into a number of arbitrarily selected increments, the number depending on the accuracy required. Experience showed that the calculations were simplified if the increments were selected at regular intervals of r_c rather than at regular intervals of volume.

The increments were considered in order from the saturation pressure. For the first increment, ΔV_1 , it was assumed

that the gas occurs due to evaporation from the capillary-condensed liquid in the largest pores. The value of ΔV_1 was corrected to standard conditions of pressure and temperature, and was recorded as the volume of gas contained in pores of the average pore radius over the first increment. For all desorption increments after the first, a correction was made for the gas volume desorbed from the walls of the pores emptied in the previous increments. This correction was made by calculating the total surface area of pores emptied of the condensed phase (the sum of the area of the pores considered in the preceding increments), and then multiplying this surface area, first, by the decrease in the number of statistical layers as the pressure was reduced, and, second, by the volume of nitrogen required to form a single layer on one square metre of surface. The sequence of the calculations was as follows:

In any increment the true pore volume, V_p , is related to the inner capillary volume, V_k , by

$$V_p = R V_k$$

where

$$R = \frac{(r_c)^2}{(r_k)^2}$$

The quantity r_k is dependent only on the relative pressure, P/P_0 . The value of r_c is dependent on the relative pressure and also on n , the number of adsorbed layers. The value of n is, in turn, also dependent on P/P_0 . To simplify the calculations, graphs of r_c , R and n as a function of P/P_0 are presented in Figures 9 and 10. The

area of the pores in any increment, A_p , is given by

$$A_p = \frac{31V_p}{\bar{r}_c},$$

where \bar{r}_c is the average pore radius in the increment over which gas is desorbed. After the first increment,

$$V_k = \Delta V - \Delta V_f$$

$$\text{where } \Delta V_f = \sum A_p \times \Delta n \times 0.23.$$

In this last equation, Δn is the decrease in the number of statistical layers as the pressure is reduced, and 0.23 is the gas volume of nitrogen to form a single layer on one square metre of surface.

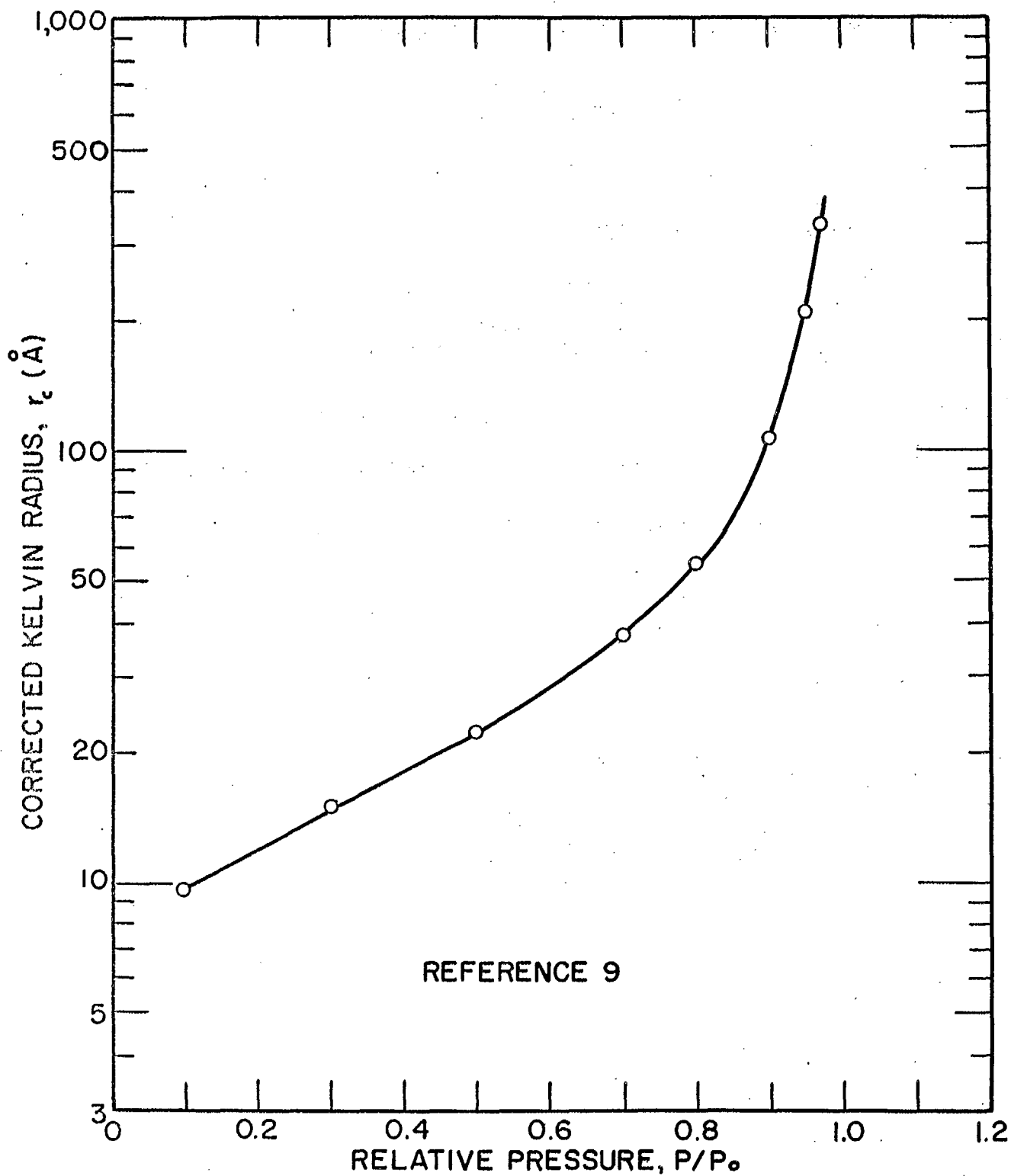


Figure 9. Plot of the corrected Kelvin radius versus the relative pressure.

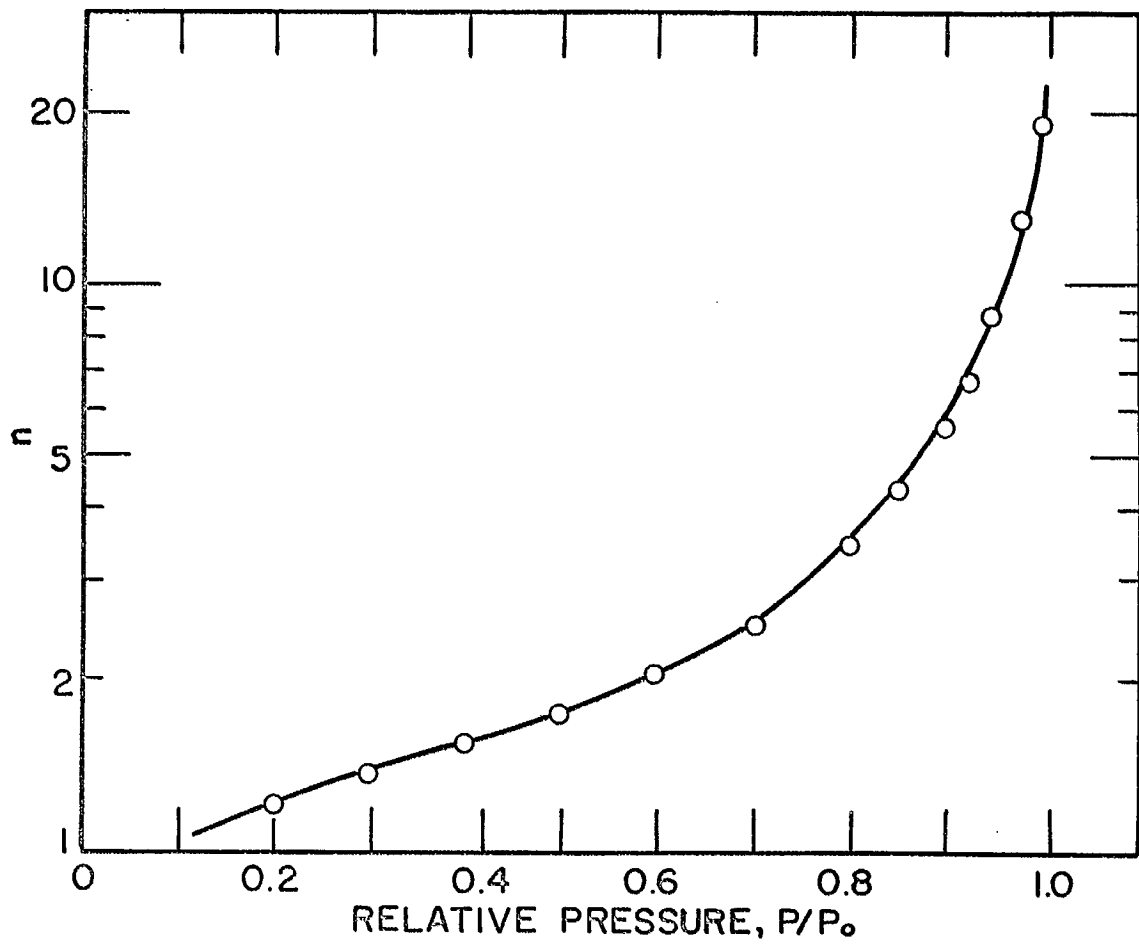
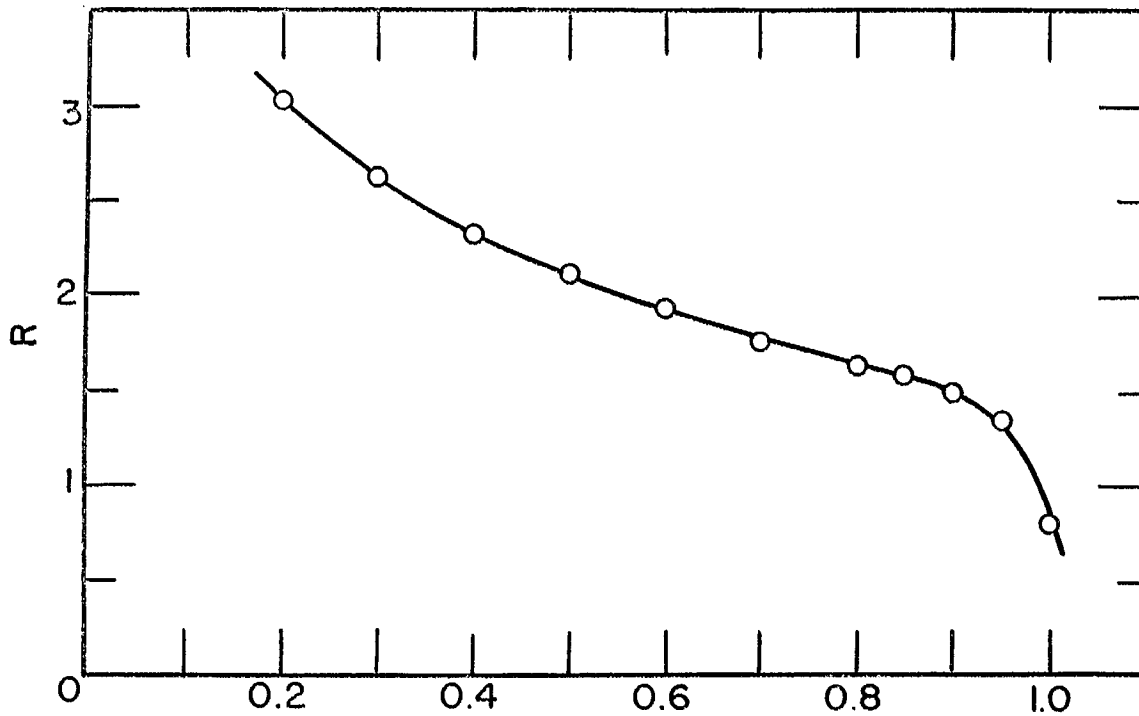


Figure 10. Graphs of n and R for the numerical integration.

RESULTS OF THE CALCULATIONS, AND DISCUSSION

The results of the three types of calculations are shown in Figures 11, 12, 13 and 14. The pore size distributions for the catalysts are presented together for easy comparison. A graph of the cumulative surface area versus the pore radius is presented in Figure 15. In the case of the synthetic alumina catalysts, most of the surface area occurs in pores of approximately 25 Å radius. In the case of the K-536 catalyst the surface area is spread more or less uniformly throughout the pore size range.

There is no doubt that the most accurate method of measuring the pore size distribution is the numerical integration proposed by Barrett, Joyner and Halenda. Any practical degree of accuracy can be attained by narrowing the limits of the increments selected for the integration. For most purposes, ten to twenty increments are adequate. Once familiarity with the system is attained, the calculations can be completed in one to two hours and the result is reliable.

The calculation technique proposed by Shull is generally faster but, because of difficulty in the fitting of the curves, there is a chance of missing a subsidiary distribution. An example of this can be seen in Figure 12, in the case of the Nalcat type S catalyst. In general, there is too great a tendency to force the data to fit a theoretical isotherm, with the result that the smaller effects pass unnoticed.

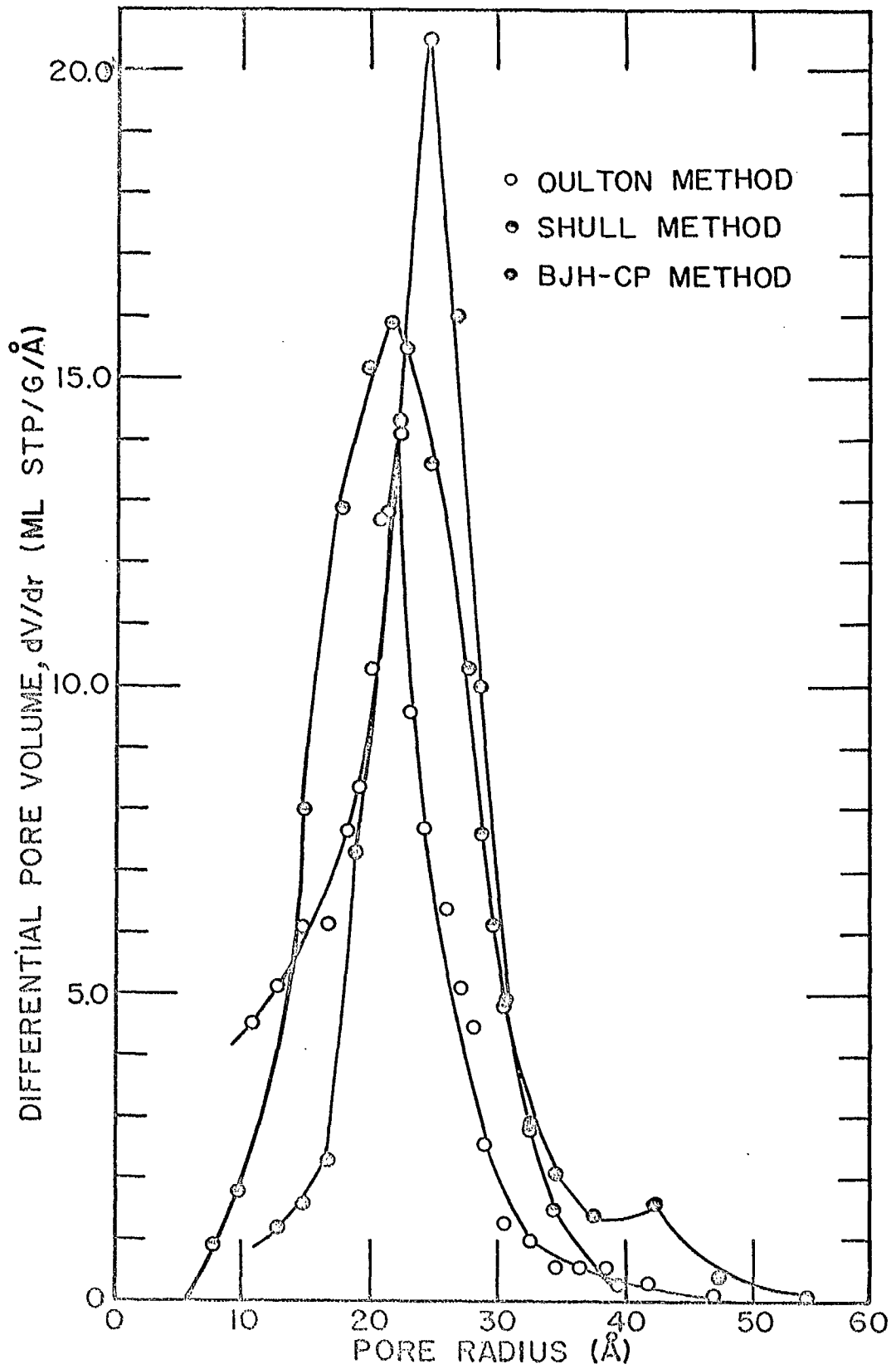


Figure 11. The pore volume distribution in the Union Oil catalyst as manufactured.

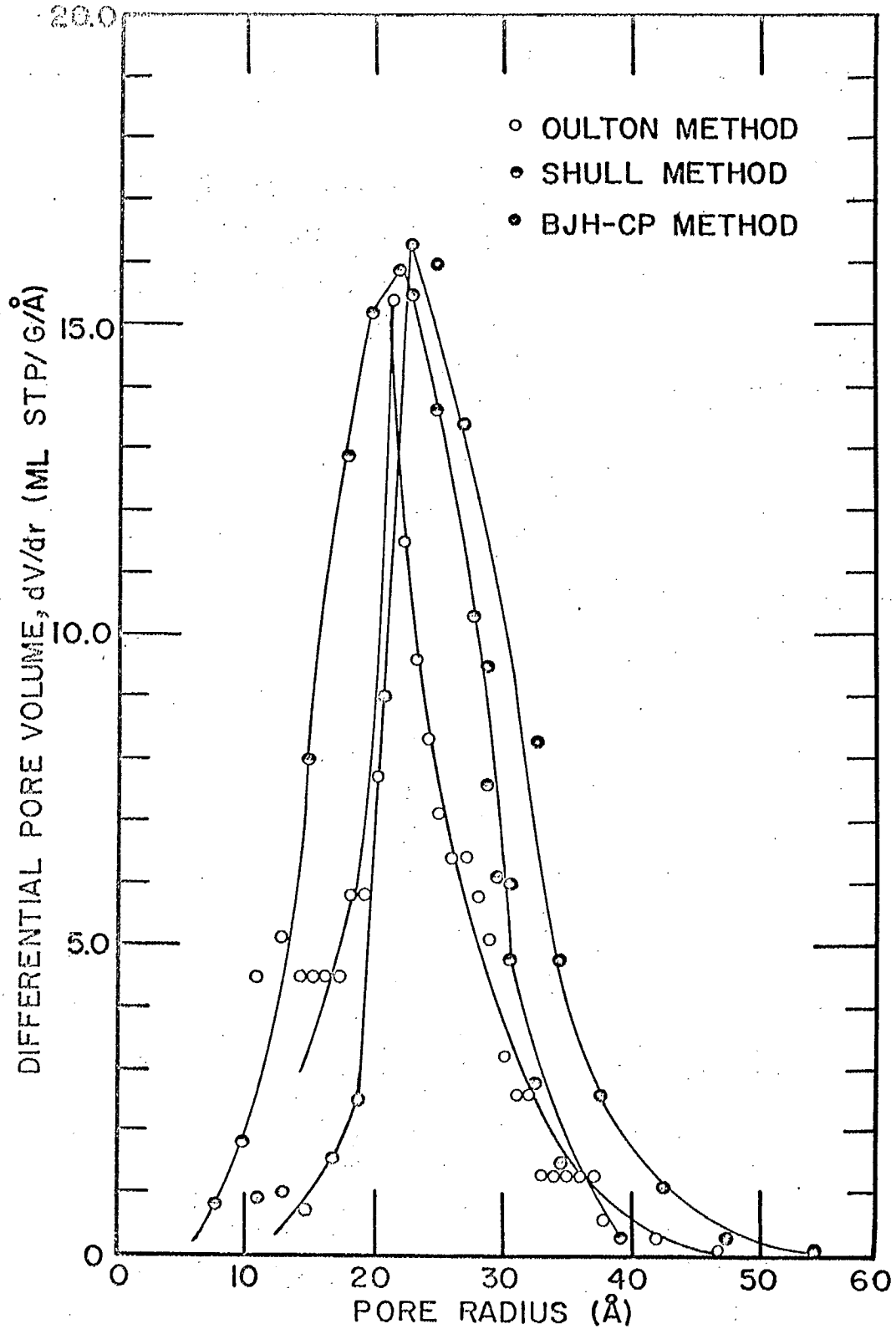


Figure 12. The pore volume distribution in the reactivated Union Oil catalyst.

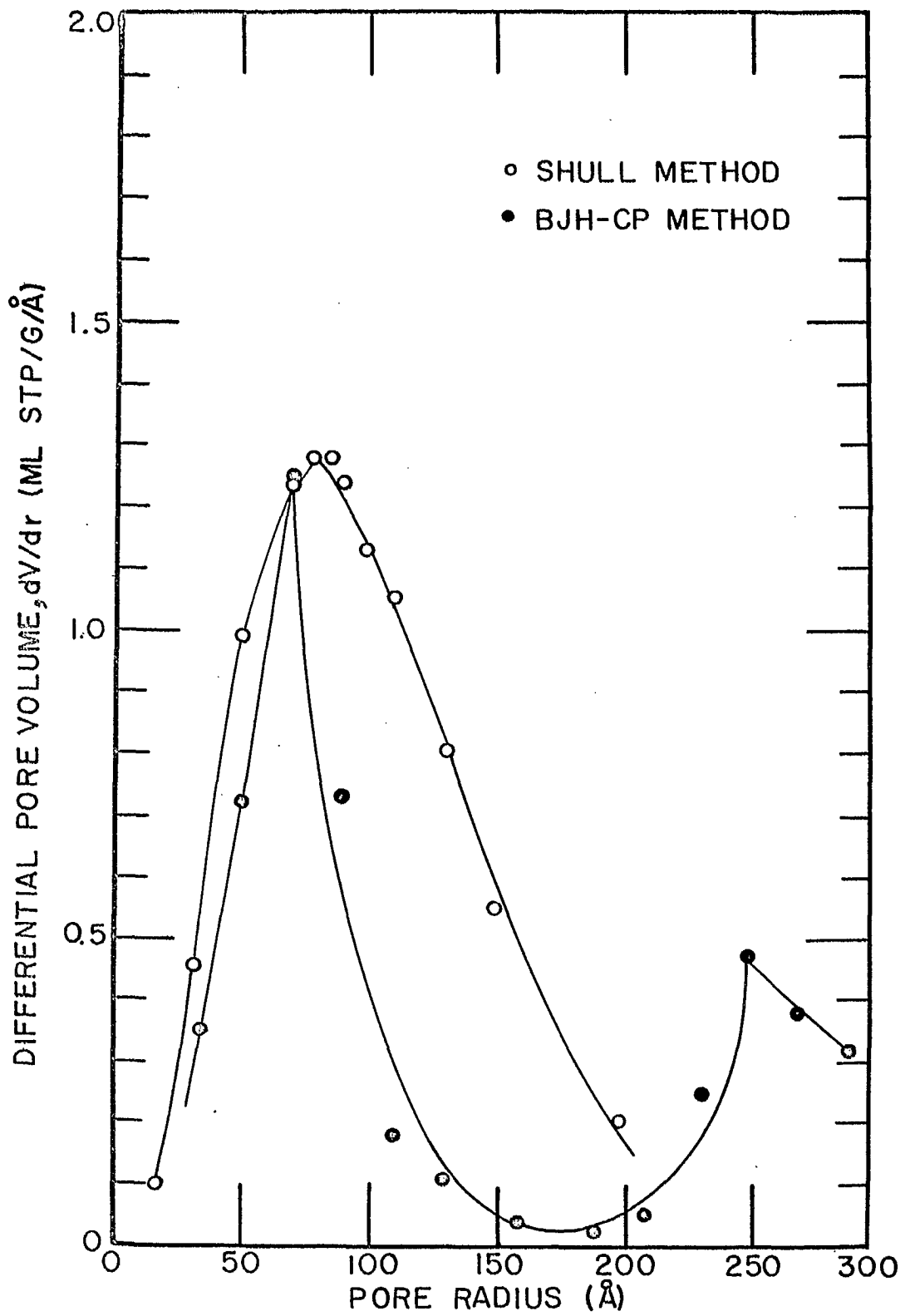


Figure 13. The pore volume distribution in the K-536 catalyst.

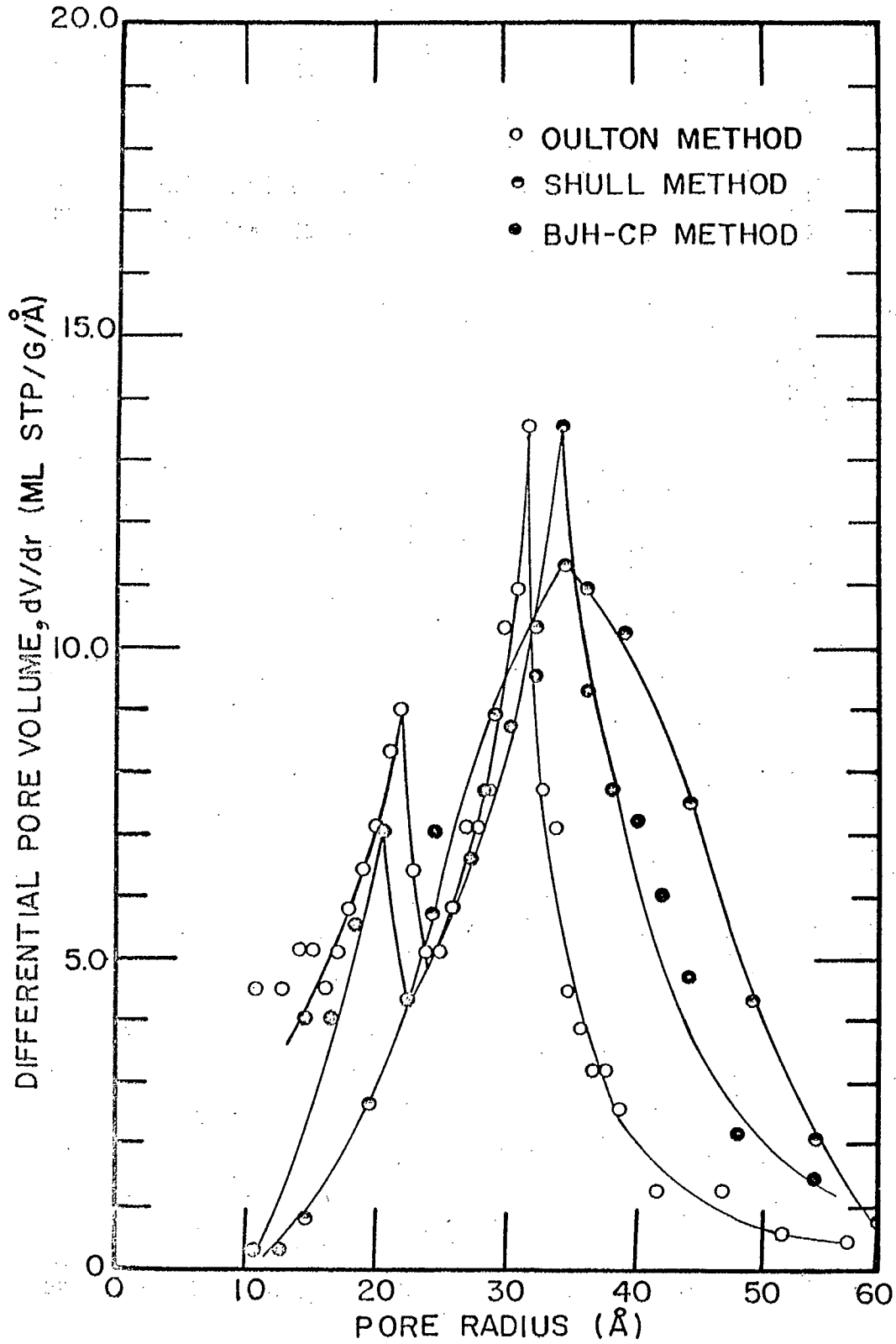


Figure 14. The pore volume distribution in the Nalcat catalyst.

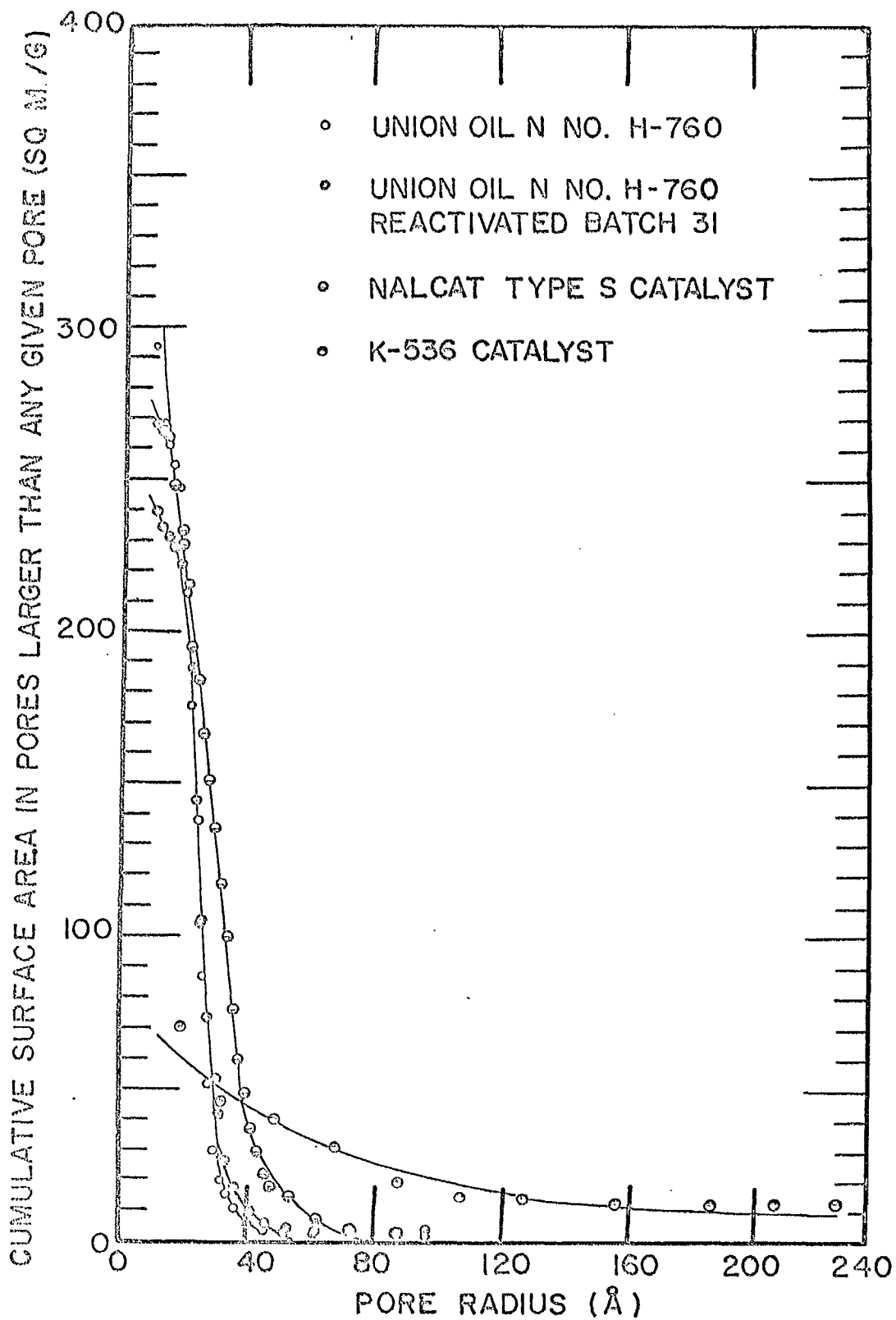


Figure 15. The surface area distribution.

Although the method attributed to Oulton is a very fast technique, it is probably the least reliable of the three calculations. Tangents can be drawn with accuracy only on isotherms of gentle slopes. Where there are rapid changes in the isotherms, similar to those encountered with the K-536 catalyst, the method cannot be used for even an approximate calculation.

There are certain types of isotherms in which the results of the various calculations are essentially identical. The type of isotherm obtained with the Union Oil cobalt molybdate catalyst gives very similar results with either the approximate tangent method or the numerical integration. Unfortunately, the only way of determining the similarity of the results obtained by the different methods is by actual calculation. A slight change in the slope, anywhere in the isotherm, can mean a subsidiary distribution which can easily be missed by either of the two simpler methods of calculation described by Oulton and Shull.

In view of the fact that the experimental determination of the isotherm requires four to five working days, it would seem practical to apply only the best method to the results. Once one is familiar with the pattern of the calculation, the arithmetic of the integration can usually be fitted into the experimental work of the next sample.

The results of the pore size determinations were very encouraging in themselves. Various qualitative tests had been made on the catalyst pellets and it was suspected that the pore size was small.

It was not known, however, that the size distribution covered such a narrow band. In the case of the cobalt molybdate catalysts, the distribution is very definitely Gaussian, with few radii greater than 50 Å.

Coking and regeneration in the pilot plant does not appear to change the pore size distribution in catalyst pellets. The sample of the regenerated cobalt molybdate catalyst studied in the present investigation had been used for the desulphurization of heavy tar sand distillates and regenerated on at least ten separate occasions. The pore size distributions before and after are very nearly identical.

REFERENCES

1. S. Brunauer, P. H. Emmett and E. Teller, J. Am. Chem. Soc. 60, 309 (1938).
2. P. H. Emmett, Measurement of the Surface Area of Solid Catalysts, in "Catalysis", Vol. I (edited by P. H. Emmett) (Reinhold Publishing Corporation, New York, 1954), p. 38.
3. W. J. Moore, "Physical Chemistry" (Prentice-Hall Publishing Co., New York, 1950), p. 488.
4. P. C. Carman, "Flow of Gases Through Porous Media" (Butterworths Scientific Publications, London, 1956), p. 44.
5. L. G. Joyner, in "Scientific and Industrial Glass Blowing and Laboratory Techniques", edited by W. E. Barr and V. J. Anhorn (Instruments Publishing Company, Pittsburgh, 1949), pp. 257-283.
6. P. E. Bugge and R. H. Kerlogue, J. Soc. Chem. Ind. 66, 377 (1947).
7. J. S. Anderson, Z. physik. Chem. 88, 191 (1914).
8. T. D. Oulton, J. Phys. Coll. Chem. 52, 1206 (1948).

9. A. Wheeler, Reaction Rates and Selectivity in Catalyst Pores, in "Catalysis", Vol. II (edited by P. H. Emmett)(Reinhold Publishing Corporation, New York, 1955), pp. 111-116.
10. C. G. Shull, J. Am. Chem. Soc. 70, 1405 (1948).
11. E. P. Barrett, L. G. Joyner and P. P. Halenda, J. Am. Chem. Soc. 73, 373 (1954).
12. C. Pierce, J. Phys. Chem. 57, 149 (1953).

BP:(PES)pg

